

PACS numbers: 79.20.Eb; 62.23.Pq; 42.82.Et; 42.55.Lt
DOI: 10.1070/QE2015v045n09ABEH015727

Formation of an ensemble of silver nanoparticles in the process of surface evaporation of glass optical waveguides doped with silver ions by the radiation of a pulsed CO_2 laser

V.I. Egorov, A.V. Nashchekin, A.I. Sidorov

Abstract. **It is shown that pulsed irradiation (a wavelength of 10.6 μm and an energy density of 0.6–8.5 J cm^{-2}) of glass with a waveguide layer containing silver ion leads to the formation of a ring, surrounding the irradiated zone and consisting of silver nanoparticles deposited on the glass surface. The possible process of formation of silver nanoparticles under laser irradiation is discussed.**

Keywords: *evaporation, CO_2 laser, glass, silver nanoparticle.*

1. Introduction

Methods of laser-induced evaporation and ablation find wide application in surface nanostructuring and producing nanoparticles of different materials [1]. These methods allow the production of dielectric [2], semiconductor [3] and metallic nanoparticles [4]. Nanoparticles of noble metals (Ag, Au, Pt) and copper, possessing plasmon resonances [5], are widely used in designing chemical sensors and biosensors based on the enhancement of luminescence [6] and Raman scattering [7]. The major effect in these cases is the local enhancement of the electromagnetic wave field amplitude under the conditions of plasmon resonance. For the synthesis of metallic nanoparticles one can use chemical reactions in liquid and polymer media [8–10], electrochemical methods [11], vacuum deposition or laser-induced ablation onto a substrate [12], ion implantation [13, 14], electron beam impact [15], thermal processing of glasses containing silver ions in reducing atmosphere [16, 17] and a number of other methods. As compared to other methods, the laser-induced evaporation and ablation of a metallic target followed by the deposition of nanoparticles onto a substrate possess a number of advantages, first of all, the simplicity and high productivity. However, silver or gold nanoparticles deposited on the substrate have low adhesion and are easily removed. The same drawback is inherent in the method of producing silver nanoparticles in reducing atmosphere [17]. In Refs [18, 19] it is shown that for the optimisation of the characteristics of a chemical sensor or biosensor, based on the nanoparticle plasmon resonance, it is necessary to isolate nanoparticles from the environment by a dielectric layer having a thickness of 5–15 nm. That is why after the synthesis the nanoparticles are coated with a layer of polymer or nonorganic material. From the point of view of sensor design, it is optimal to produce metallic nanoparticles on the surface of optical waveguides or fibres [20, 21]. This increases the efficiency and simplifies the collection of the analysed radiation, as well as allows the fabrication of sensor matrices in the form of biochips.

Based on the above considerations, the aim of the present work was formulated, namely, to study the possibility of producing silver nanoparticles by means of laser-induced evaporation from the surface of silicate glass waveguides containing silver ions and to analyse the specific features of this process. It was assumed that the laser-induced evaporation should not cause essential distortion of the waveguide optical characteristics (formation of craters, glass cracking, etc.). Therefore, the energy density range of the incident radiation was chosen to be minimal.

2. Experimental technique

In the experiments we used polished plates of sodium silicate glass with the composition $SiO_2–Na_2O–MgO–Al_2O_3–CaO$. The silver ions were injected into the near-surface layers of the glass using the ion exchange method $Ag^+ \rightarrow Na^+$ [22] in the melt of the $AgNO_3$ (5 mol %) + $NaNO_3$ (95 mol %) mixture at the temperature 350 °C during 15 min. The calculation shows that under such ion exchange conditions silver ions penetrate into the glass to the depth of 20 μm. In the near-surface glass layer a gradient planar waveguide is formed [22]. The glass was exposed to focused radiation of a 10.6-μm pulsed waveguide CO_2 laser (Syngrad). The irradiation was performed with single laser pulses in air at the atmospheric pressure. The diameter of the irradiated glass zone was measured to be 100 μm. The mean energy density E in the irradiated zone varied from 0.6 to 8.5 J cm^{-2}. The laser pulse duration was 40–150 μs. For measuring the optical density spectra, the samples were fabricated, in which the irradiated zones formed an array of regularly arranged 'points' (see the inset in Fig. 1a) filling an area of 2×2 mm. The optical density spectra in this case are integral and represent a sum of spectra of the initial glass, the rings and the irradiated zones. The optical density spectra were measured using a Lambda spectrophotometer (PerkinElmer) at room temperature. Electron microscope images were obtained using a JSM 7001F (JEOL) scanning electron microscope (SEM).

V.I. Egorov, A.I. Sidorov ITMO University, Kronverkskii prosp. 49, 197101 St. Petersburg, Russia; e-mail: egorovvl@gmail.com, aisidorov@qip.ru;
A.V. Nashchekin Ioffe Institute, Russian Academy of Sciences, ul. Politekhnicheskaya 26, 194021 Saint-Petersburg, Russia; e-mail: nashchekin@mail.ioffe.ru

Received 6 December 2014; revision received 2 February 2015
Kvantovaya Elektronika **45** (9) 858–862 (2015)
Translated by V.L. Derbov

3. Experimental results and discussion

The experiments have shown that the effect of a CO_2 laser pulse with $E = 0.6–8.5$ J cm^{-2} on the glass containing silver ions leads to the appearance of a ring around the irradiated zone (Fig. 1a) with the colour varying from light yellow to brown with the growth of energy density. The width of the ring amounts to 15–20 μm. At $E = 0.95–8.5$ J cm^{-2} the colouring also appears directly in the irradiated zone. The SEM image of the irradiated zone at $E = 0.95$ J cm^{-2} (Fig. 1c) shows that at this energy density the damage of the glass surface by the laser radiation is minimal. (The defect in the left-hand part of the Figure is not related to the effect of the laser pulse and is a result of the separation of the metallic film, deposited onto the surface to remove the surface charge in the process of scanning with the electron beam.) At $E \geqslant 3.8$ J cm^{-2} a crater is formed in the centre of the irradiated zone (Figs 1b and 1d), and around the irradiated zone the glass cracking appears due to mechanical and thermal stresses. In this case the ring is a continuous film of metallic silver with a high reflection coefficient that can be observed visually (Fig. 1b). Figure 1d shows the SEM image of a crater in the glass after the impact of a laser pulse with $E = 8.5$ J cm^{-2}. It is seen that as a result of the glass melt slopping, a swell is formed along the crater perimeter. Two concentric rings can be seen at the inner part of the swell, which are the result of melted glass wave motion. Dark points are present in the central part of the crater, which are bubbles of air that appeared in the process of glass boiling. Such modifications of the surface will obviously cause essential worsening of the waveguide optical characteristics.

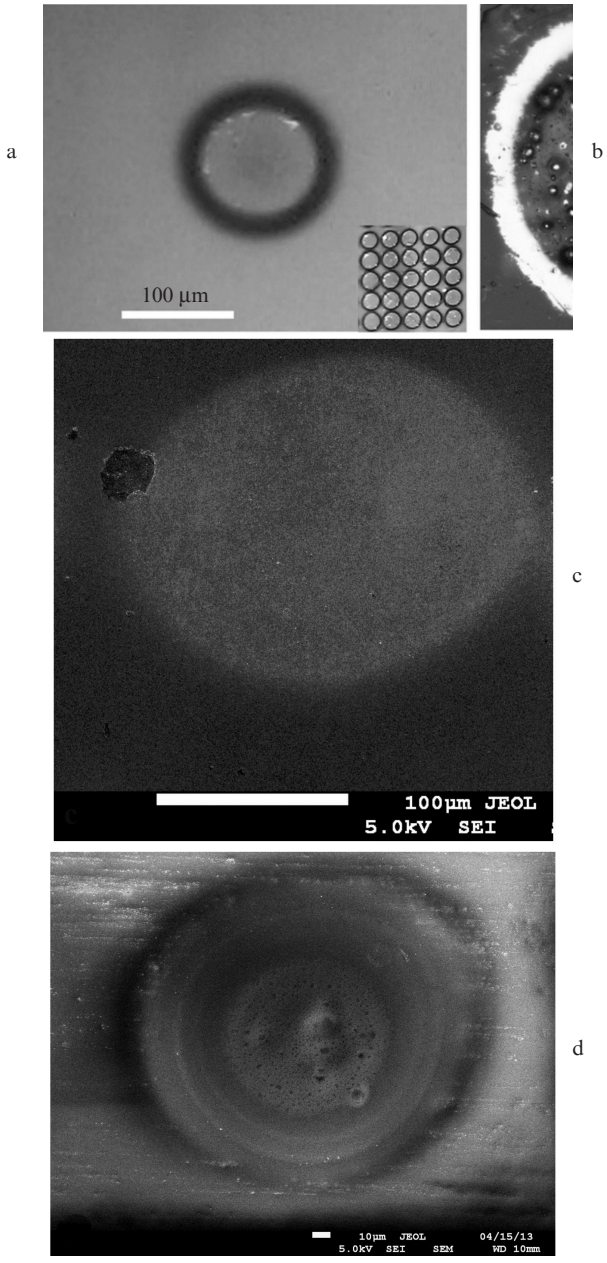

Figure 1. Photographs of (a) the irradiated glass zone at $E = 0.95$ J cm^{-2} (the inset shows a fragment of the matrix used for measuring the integral optical density) and (b) the edge of the irradiated glass zone at $E = 8.5$ J cm^{-2}, as well as SEM images of (c) the irradiated zone at $E = 0.95$ J cm^{-2} and (d) a crater at $E = 3.8$ J cm^{-2}. The photographs in Figs 1a and 1b are obtained in reflected light using an optical microscope.

The integral spectra of the glass optical density after the CO_2 laser irradiation are shown in Fig. 2. It is seen that the irradiation of the glass with the CO_2 laser leads to the appearance of absorption bands in the spectral intervals 370–380 nm and 400–500 nm. With increasing E, the maximum of the longer wavelength absorption band is shifted from $\lambda = 430$ to 445 nm. It is known [5, 23] that the isolated spherical uncoated nanoparticles of silver with the diameter 2–20 nm possess relatively narrow plasmon absorption bands in the spectral interval 390–400 nm. The absorption bands shown in Fig. 2 are characteristic for plasmon absorption bands of silver nanoparticles in the following cases:

1) the nanoparticles have the shape, different from the spherical one, e.g., the shape of an ellipsoid [5];

2) the separation between the nanoparticles is smaller than 20 nm, i.e., they are to be considered as an ensemble of nanoparticles with electromagnetic interaction [5, 9];

3) the additional electromagnetic interaction between the nanoparticles, separated by relatively large distances (as in our case), arises as a result of the excitation of modes in the waveguide layer located near the glass surface [21, 24];

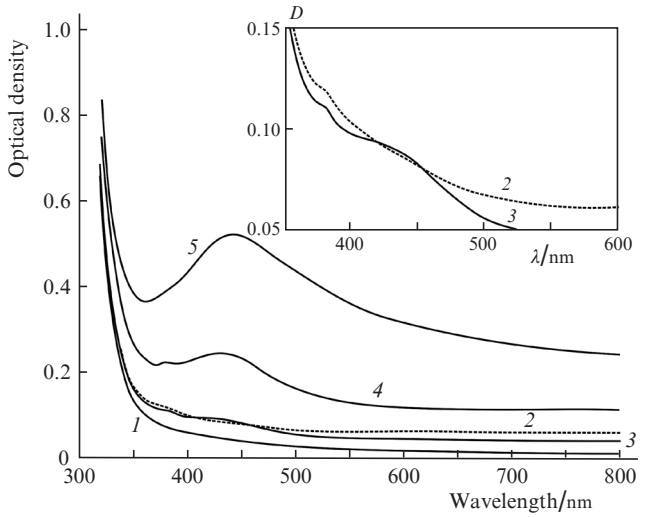

Figure 2. Spectra of the integral optical density D of the glass before (*1*) and after the irradiation with the CO_2 laser with $E =$ (*2*) 0.6, (*3*) 0.95, (*4*) 3.8 and (*5*) 8.5 J cm^{-2}. The inset shows curves (*2*) and (*3*) in the magnified scale.

4) the size of a nanoparticle is greater than 20 nm, i.e., the nanoparticle is already a multipole, which leads to additional plasmon resonances [5]; and

5) the metallic particle has a dielectric coating, so that the plasmon absorption band is shifted towards longer wavelengths [5].

Figure 3 shows the SEM image of silver nanoparticles at the outer side of the ring around the irradiated zone. Allowing for the fact that the nanoparticles are located at the waveguide surface, it is seen that the optical density spectra are affected by four of the above factors. Below it will be shown that a dielectric coating is formed on the surface of silver nanoparticles. Therefore, this factor also affects the position of the plasmon absorption band. The size of the nanoparticles varies from 10 to 100 nm. Many of them have the shape close to spherical, but a number of nanoparticles have the shape of prolate ellipsoids. The separation between them in some places does not exceed 10 nm. From Fig. 3 it is also seen that the nanoparticles having the shape of ellipsoids are similarly oriented, so that their long axes are oriented along the direction of the laser-induced torch plasma expansion.

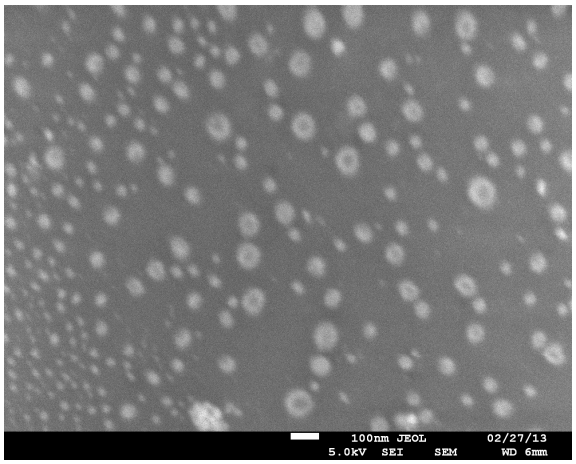

Figure 3. SEM image of silver nanoparticles at the outer side of the ring at $E = 3.8$ J cm^{-2}.

Figure 4 shows the normalised size distribution of nanoparticles at the outer side of the ring. It is seen that the nanoparticles with the diameter 10–15 nm have the maximal surface concentration. The increase in the nanoparticle diameter is accompanied by a decrease in their concentration. The shape of the nanoparticle size distribution envelope is close to exponential.

For a wavelength of 10.6 μm the relevant absorption band of silicate glasses lies within the interval 1800–2000 cm^{-1} [25]. The calculation shows that in the layer of silicate glass with the thickness 3–4 μm, 50% of radiation power at this wavelength is absorbed. It is known that the boiling temperature of sodium-doped silicate glasses varies within the interval 1800–1900 °C depending on the composition. To estimate the upper boundary of the surface heating under the conditions of our experiments, the laser irradiation of silica glass (the boiling temperature 2230 °C) was performed that did not cause the evaporation of the surface layer. From this result we conclude that the temperature of the glass surface heating is limited by the above values. The evaporated components of glass, including the silver, form a torch that absorbs a fraction

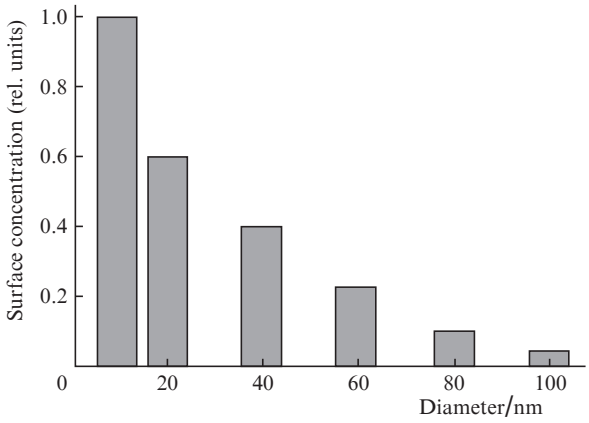

Figure 4. Normalised size distribution of silver nanoparticles at the outer side of the ring.

of laser radiation. The heating of the torch in the laser beam leads to the thermal ionisation of its components [26] and to the formation of plasma, the presence of which is confirmed by the white-blue glow of the interaction region during the laser pulse.

At the torch boundaries the recombination of electrons and ions and the deposition of the glass components around the irradiated zone can occur. However, the small time of the laser pulse action (100 μs) and relatively low temperature of the glass around the irradiated zone do not provide the possibility of formation of silver nanoparticles by means of the diffusion of silver atoms over the glass surface. The process is also hampered by fast cooling of the irradiated zone. According to Ref. [2], the cooling rate of the irradiated zone of a dielectric after the termination of the CO_2 laser pulse action amounts to nearly 1.3 K μs^{-1}, so that the only possible mechanism of silver nanoparticle formation during the laser pulse is the formation at the torch boundaries, where the concentration and mobility of silver atoms are relatively high. At the final stage of the laser pulse action and after it, as a result of the torch temperature decrease, nanoparticles are formed in its central part, which is confirmed by the appearance of colouring in the central part of the irradiated zone. It is worth noting that, in spite of the complex chemical composition of the glass, nanoparticles produced at the torch boundaries consist of pure silver rather than of its chemical compounds, e.g., silver silicates. The possible reason is the instability of most chemical compounds of silver, which are easily decomposed at high temperature.

Consider now the probability of the laser-induced formation of silver nanoparticles under the glass surface, e.g., in the crater region. It is known (see, e.g., [27]) that in sodium silicate glasses with neutral silver atoms in the course of thermal processing at a temperature insignificantly exceeding the temperature of vitrification T_g (T_g = 480–560 °C depending on the glass composition), the formation of silver nanoparticles occurs as a result of thermal diffusion of silver atoms. The duration of thermal processing in this case is 1–10 h. Silver ions cannot form a nanoparticle because of the Coulomb repulsion. At essentially higher temperatures, e.g., greater than 900 °C, an opposite process occurs, namely, the dilution of silver nanoparticles in the glass with the transition of silver into the atomic state. In our experiments the silver inside the glass was initially in the ion state. The glass heating or melting, the case when there are special reducing dopants, does

not give rise to free electrons. The high temperature in the crater region and fast cooling of the irradiated zone after the laser pulse inhibit the formation of nanoparticles in the glass even if the neutral silver atoms appear. Thus, we can conclude that the pulsed CO_2 laser irradiation cannot lead to the formation of silver nanoparticles inside the near-surface layer of the glass.

To confirm the above conclusions the following experiment was carried out. The radiation of the CO_2 laser was focused on the glass substrate with silver ions through the polished plates of single-crystal KBr or ZnSe (Fig. 5a), transparent in the 10-μm spectral region. The plates were placed directly on the surface of the glass substrate. As a result of exposure, the circles and rings appeared at the surface of KBr and ZnSe plates, adjacent to the glass substrate (Figs 5b and 5c), similar to those at the surface of the grass substrate. The fact that the 'reprint' at the ZnSe plate is weaker than that at the KBr plate may be explained by the smaller energy of the incident radiation [because of the high (n = 2.5) refractive index of ZdSe, the coefficient of Fresnel reflection from two plate faces amounts to 30%]. The spectral measurements have shown that in the optical density spectra (Fig. 6) of the plates the plasmon absorption bands appear, similar to those shown in Fig. 2. Thus, this experiment confirms that the formation of silver nanoparticles occurs directly at the boundaries of the laser torch during the laser pulse action and inside the torch after the pulse action end.

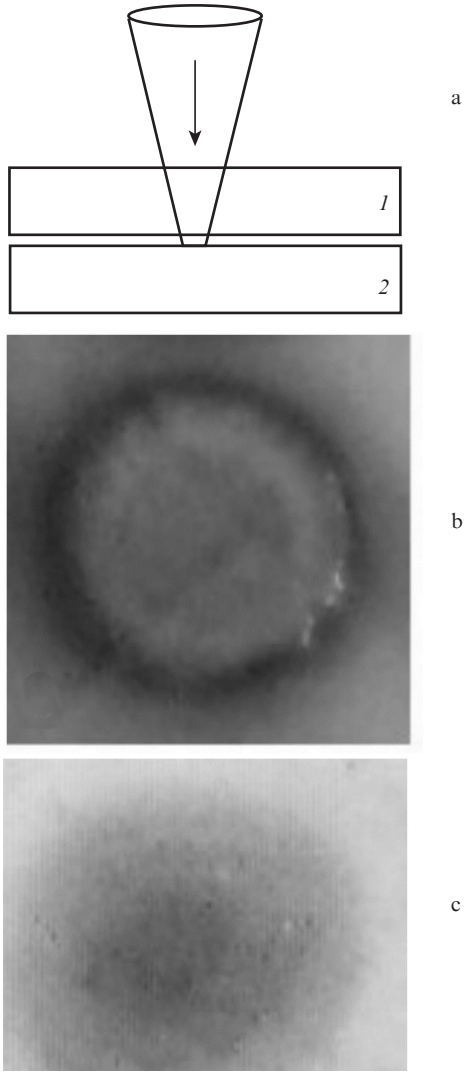

Figure 5. (a) Schematic diagram of irradiation of the glass with the CO_2 laser [(*1*) KBr or ZnSe plate, (*2*) glass doped with silver ions] and a photograph of the laser torch trace on the plates of (b) KBr and (c) ZnSe. The photographs were obtained in reflected light; E = 3.8 J cm^{-2}.

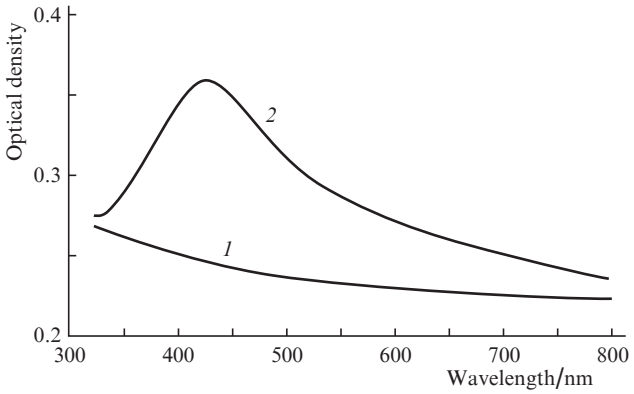

Figure 6. Spectra of integral optical density of KBr plate (*1*) before and (*2*) after irradiation of the glass doped with silver ions with a CO_2 laser; E = 3.8 J cm^{-2}.

The deposition of silver nanoparticles at the glass surface around the irradiated zone is accompanied by the deposition of other dielectric components of glass, which provide firm fixation of nanoparticles on the glass surface and form a dielectric coating of the nanoparticles. The removal of nanoparticles from the glass surface is possible only using mechanical grinding or polishing. The main components of the coating can be silicon oxides (the basic component of the silicate glass) and silicon nitrides (irradiation is performed in air). To check it, the glass after the exposure to CO_2 laser radiation was etched in a 10% aqueous solution of HNO_3 during 15 min. The etching did not lead to the disappearance of plasmon absorption bands of silver nanoparticles. The control experiment has shown that a silver film with a thickness of 100 nm on the glass surface is diluted by a similar HNO_3 solution in less than 5 min. Since silicon oxides and nitrides are solvable in hydrofluoric acid, the etching of irradiated samples in a 2.5% aqueous solution of HF was carried out during 2–4 s at room temperature, after which the samples were washed in water. After this procedure the nanoparticles could be easily removed from the surface with cloth or water jet. This confirms the hypothesis about the appearance of a dielectric buffer layer on the surface of silver nanoparticles. The experiment allows a rough estimate of the thickness of the dielectric layer coating nanoparticles as smaller than 50 nm.

4. Conclusions

The impact of pulsed CO_2 laser radiation on the glass optical waveguide containing silver ions in the interval of energy densities 0.6–8.5 J cm^{-2} leads to the formation of silver nanoparticles at the boundaries of the laser torch. The particles are deposited on the waveguide surface, forming a ring around the irradiated zone. The size of nanoparticles amounts to 10–100 nm. The dielectric components of the glass, deposited

on the surface from the torch, form a protective coating on the silver nanoparticles, fixing them on the waveguide surface. The 'soft' regime of irradiation of the glass allows one to avoid the glass cracking, crater formation and essential worsening of the waveguide optical characteristics.

Acknowledgements. The work was supported by the Russian Science Foundation (Agreement No. 14-23-00136).

References

1. Zavestovskaya I.N. *Kvantovaya Elektron.*, **40**, 942 (2010) [Quantum Electron., **40**, 942 (2010)].
2. Osipov V.V., Platonov V.V., Lisenkov V.V. *Kvantovaya Elektron.*, **39**, 541 (2009) [*Quantum Electron.*, **39**, 541 (2009)].
3. Bulgakov A.V., Evtushenko A.B., Shukhov Yu.G., Ozerov I., Marin V. *Kvantovaya Elektron.*, **40**, 1021 (2010) [*Quantum Electron.*, **40**, 1021 (2010)].
4. Amoruso S., Ausanio G., Bruzzese R., Vitiello M., Wang X. *Phys. Rev. B*, **71**, 033406 (2005).
5. Klimov V.V. *Nanoplasmonics* (Boca Raton, USA: CRC Press, 2014; Moscow: Fizmatlit, 2009).
6. Eichelbaum M., Rademann K. *Adv. Funct. Mater.*, **19**, 1 (2009).
7. Chen Y., Jaakola J.J., Saynatjoki A., Tervonen A., Honkanen S. *J. Raman Spectrosc.*, **42**, 936 (2011).
8. Dykman L.A., Bogatyrev V.A., Shchegolev S.Yu., Khlebtsov N.G. *Zolotye nanochastitsy: sintez, svoystva, biomeditsinskoye primeneniye* (Gold Nanoparticles: Synthesis, Properties, Biomedical Applications) (Moscow: Nauka, 2008).
9. Karpov S.V., Slabko V.V. *Opticheskiye i fotofizicheskiye svoystva fraktal'no-structurirovannykh zoley metallov* (Optical and Photophysical Properties of Fractal-Structured Sols of Metals) (Novosibirsk: Izd-vo SO RAS).
10. Shang L., Dong S., Nienhaus G.U. *Nano Today*, **6**, 401 (2011).
11. Gonzalez B.S., Rodriguez M.J., Blanco C., Rivas J., Lopez-Quintela M.A., Martinho J.M.G. *Nano Lett.*, **10**, 4217 (2010).
12. Boltayev A.P., Penin N.A., Pogosov A.O., Pudonin F.A. *Zh. Eksp. Teor. Fiz.*, **123**, 1067 (2003) [*JETP*, **96**, 945 (2003)].
13. Ganeev R.A., Ryasnyanskii A.I., Stepanov A.L., Kondirov M.K., Usmanov T. *Opt. Spektrosk.*, **95**, 1034 (2003) [*Opt. Spectrosc.*, **95** (6), 967 (2003)].
14. Stepanov A.L. *Rev. Adv. Mater. Sci.*, **4**, 45 (2003).
15. Ignat'ev A.I., Nashchekin A.V., Nevedomskii V.M., Podsvirov O.A., Sidorov A.I., Solovyov A.P., Usov O.A. *Zh. Tekh. Fiz.*, **81**, 75 (2011) [*Tech. Phys.*, **56** (5), 662 (2011)].
16. Kaganovskii Yu., Mogilko E., Lipovskii A.A., Rosenbluh M. *J. Phys.: Conf. Ser.*, **61**, 508 (2007).
17. Obraztsov P.A., Nashchekin A.V., Nikonorov N.V., Sidorov A.I., Panfilova A.V., Brunkov P.N. *Fiz. Tverd. Tela*, **55**, 1180 (2013) [*Phys. Solid State*, **55** (6), 1272 (2013)].
18. Guzatov D.V., Vaschenko S.V., Stankevich V.V., Lunevich A.Y., Glukhov Y.F., Gaponenko S.V. *J. Phys. Chem.*, **116**, 10723 (2012).
19. Anger P., Bharadwaj P., Novotny L. *Phys. Rev. Lett.*, **96**, 113002 (2006).
20. Février M., Gogol P., Aassime A., Mégy R., Delacour C., Chelnokov A., Apuzzo A., Blaize S., Lourtioz J.-M., Dagens B. *Nano Lett.*, **12**, 1032 (2012).
21. Cheng T., Rangan C., Sipe J.E. *J. Opt. Soc. Am. B*, **30**, 743 (2013).
22. Tervonen A., West B.R., Honkanen S. *Opt. Eng.*, **50**, 071107 (2011).
23. Kriebig U., Vollmer M. *Optical Properties of Metal Clusters* (Berlin: Springer-Verlag, 2010).
24. Soller B., Hall D. *J. Opt. Soc. Am. B*, **19**, 2437 (2002).
25. Zolotarev V.M., Morozov V.N., Smirnova E.V. *Opticheskiye postoyannye prirodnykh i tekhnicheskikh sred. Spravochnik* (Optical Constants of Natural and Technical Media. A Handbook) (Leningrad: Khimiya, 1984).
26. Koroteyev N.I., Shumay I.L. *Fizika moshchnogo lazernogo izlucheniya* (Physics of High-Power Laser Radiation) (Moscow: Nauka, 1991).
27. Nikonorov N.V., Sidorov A.I., Tsekhomskii V.A. In: *Silver nanoparticles*. Ed. by D.P. Perez (Vukovar: In–Tech, 2010).